Quantitative proteomics reveal the alterations in the spinal cord after myocardial ischemia-reperfusion injury in rats

SHUN-YUAN LI[1], ZHI-XIAO LI[2], ZHI-GANG HE[3], QIAN WANG[2], YU-JUAN LI[2], QING YANG[4], DUO-ZHI WU[5], HAO-LONG ZENG[6] and HONG-BING XIANG[2]

[1]Department of Anesthesiology, The First Affiliated Quanzhou Hospital of Fujian Medical University, Quanzhou, Fujian 362000; Departments of [2]Anesthesiology and Pain Medicine, and [3]Emergency Medicine, Tongji Hospital of Tongji Medical College, Huazhong University of Science and Technology, Wuhan, Hubei 470030; [4]College of Life Science, Wuhan University, Wuhan, Hubei 430076; [5]Department of Anesthesiology, Hainan General Hospital, Haikou, Hainan 570311; [6]Department of Laboratory Medicine, Tongji Hospital, Tongji Medical College, Huazhong University of Science and Technology, Wuhan, Hubei 470030, P.R. China

Received April 19, 2019; Accepted August 6, 2019

DOI: 10.3892/ijmm.2019.4341

Abstract. There is now substantial evidence that myocardial ischemia-reperfusion (IR) injury affects the spinal cord and brain, and that interactions may exist between these two systems. In the present study, the spinal cord proteomes were systematically analyzed after myocardial IR injury, in an attempt to identify the proteins involved in the processes. The myocardial IR injury rat model was first established by cross clamping the left anterior descending coronary artery for 30-min ischemia, followed by reperfusion for 2 h, which resulted in a significant histopathological and functional myocardial injury. Then using the stable isotope dimethyl labeling quantitative proteomics strategy, a total of 2,362 shared proteins with a good distribution and correlation were successfully quantified. Among these proteins, 33 were identified which were upregulated and 57 were downregulated in the spinal cord after myocardial IR injury, which were involved in various biological processes, molecular function and cellular components. Based on these proteins, the spinal cord protein interaction network regulated by IR injury, including apoptosis, microtubule dynamics, stress-activated signaling and cellular metabolism was established. These heart-spinal cord interactions help explain the apparent randomness of cardiac events and provide new insights into future novel therapies to prevent myocardial I/R injury.

Correspondence to: Professor Hong-Bing Xiang, Department of Anesthesiology and Pain Medicine, Tongji Hospital of Tongji Medical College, Huazhong University of Science and Technology, 1095 Jiefang Avenue, Wuhan, Hubei 470030, P.R. China
E-mail: hbxiang@tjh.tjmu.edu.cn

Dr Hao-Long Zeng, Department of Laboratory Medicine, Tongji Hospital, Tongji Medical College, Huazhong University of Science and Technology, 1095 Jiefang Avenue, Wuhan, Hubei 470030, P.R. China
E-mail: zenghaolongtjh@163.com

Key words: myocardial ischemia-reperfusion injury, spinal cord, proteomics, gene ontology analysis, protein interaction network

Introduction

There is increasing evidence that nociceptive signals trigger the neuronal excitation of the spinal cord. For instance, mechanical and cooling stimuli induced by spinal nerve ligation results in the alteration of spinal 5-hydroxytryptophan (HT) receptors (1), which are involved in descending pain facilitation and inhibition (2-4). There is unequivocal agreement on the important role of cardiac-spinal cord reflexes in physiological and pathophysiological conditions (5,6). Cardiac ischemia induces the release of some chemical mediators including bradykinin, protons and reactive oxygen species in the epicardium (7-10), which activate cardiogenic sympathetic afferents projecting to the upper thoracic spinal cord (11-14), resulting in the release of substance P and calcitonin gene-related peptide into the spinal cord (15-20). Studies on the mechanism of heart-spinal cord neural crosstalk have given attractive prospects in recent years (21-24). Accumulating evidence has shown that the thoracic spinal cord exerts an important role during myocardial ischemia-reperfusion injury. A case report demonstrated that spinal cord stimulation effectively alleviated chest pain caused by myocardial ischemia, which revealed that the spinal cord mechanism may be involved in cardioprotection (25). Moreover, a study by Southerland *et al* (26) found that ischemia-reperfusion injury can be alleviated through adrenergic neurons, resulting in myocardial protection by prior application of spinal cord stimulation. Jiang *et al* and Lu *et al* (27-29) found that pretreatment with intrathecal opioids attenuated myocardial ischemia-reperfusion injury, which may be associated with nitric oxide synthase activation. Myocardial reperfusion injury can be attenuated by ischemic preconditioning (IPC) (30). Using functional MRI, Huang *et al* (31) revealed that the nociceptive-related neuronal activity of the spinal dorsal horn was decreased in the IPC group. Therefore, demonstrating the

mechanisms between heart and spinal cord has become a focal point that deserves further study. However, there are still many challenges remaining for systemic clarification of the spinal mechanisms after myocardial ischemia-reperfusion injury, as a number of underlying details still remain poorly understood.

Rapid advancements in high-throughput technologies and computational frameworks offer an excellent opportunity to quantify spinal nociception using neuronal activation induced by noxious stimuli. The author's previous study showed that transcriptomics and metabolomics enable the examination of spinal biological systems in unprecedented detail (32-36). More recently, different patterns were revealed in the metabolic and transcriptional levels of the thoracic spinal cord under myocardial ischemia-reperfusion injury (37-39). Variations in metabolomics and transcriptomics are closely related to proteomics. This study was designed to further explore the differentially expressed proteins in the thoracic spinal cord after myocardial ischemia-reperfusion injury. Up to now, proteomics has been shown to be able to robustly detect various proteins with diverse biological functions in the brain and spinal cord (40,41), offering new clues for central molecular mechanisms with greater spatial and temporal coverage. In this study, the spinal cord proteomes were systematically analyzed after myocardial ischemia-reperfusion (IR) injury, attempting to identify the proteins involved in the processes.

Materials and methods

Animals. A total of 30 adult male Sprague-Dawley rats (250-300 g) were provided by the Experimental Animal Center of Tongji Medical College, Huazhong University of Science and Technology. All surgical and experimental procedures were performed according to the guidelines of the Huazhong University of Science and Technology Guide for the Care and Use of Laboratory Animals (TJ-A20150804). The rats were maintained and habituated under controlled conditions (12-h light-dark cycles, 22˚C±0.5˚C, relative humidity, 40-60%, with free access to food and drinking).

Myocardial IR injury. Rats were randomly divided into sham and model groups (n=9 in each group). To induce myocardial IR injury, a previously reported procedure was followed (37,42). rats were anesthetized with pentobarbital sodium (30 mg/kg, intraperitoneal). Before intratracheal intubation, rats were maintained with 2% isoflurane in 100% oxygen in an anesthetic chamber until losing righting reflex. After intubation, continuous 2% isoflurane in 100% oxygen were given and a small animal ventilator (tidal volume at 2.5 ml/100 g and a respiration rate 80/min) was used to control the respiration of the animal during the surgical procedure. The chest was opened via the third intercostal space, then the left anterior descending artery (LAD) was ligated with 6-0 silk suture via a silicon tube. A paleness in the appearance in the ischemic myocardium was one proof of a successful LAD ligation. After 30-min ischemia, the ligation was released and the silicon tube was removed, then the reperfusion for 2 h was initiated. Sham rats were operated as the model group but without LAD ligation. The serum cardiac troponin I (cTnI) concentration was used to detect myocardial injury and values are presented as the mean ± standard error of the mean (SEM; n=4 rats per group, Mann-Whitney U test).

Extraction and digestion of spinal cord proteins. According to Hickman's method (43), rats were decapitated before tissue harvest, which was considered a common physical method for euthanasia. Normally, pulse oxygen saturation, respiration rate or heartbeats were used to verify death, prior to tissue collections. Spinal cord segments between T1 and T4 were obtained from the operated spinal cord area of the IR rats and sham rats. Tissues were washed in PBS, directly frozen in liquid nitrogen and stored at -80˚C until further use.

For proteomics experiments, tissues from each rat were homogenized individually with a douncer in RIPA buffer containing various protease inhibitors (25 mM Tris-HCl pH 7.6, 150 mM NaCl, 1% NP-40, 1% sodium deoxycholate, 0.1% SDS, 1 mM NaF, 1 mM Na_3VO_4, with an added protease inhibitor cocktail mixture, COMPLETE; Roche Applied Science). The homogenates were held at 4˚C for 30 min and then centrifuged at 12,000 x g for 30 min at 4˚C. The supernatants were collected for the following in-solution digestion.

The in-solution digestion was performed as described previously with minor modifications (40). Briefly, proteins were precipitated and re-suspended with 8 M urea/4 mM $CaCl_2$/0.2 M Tris-HCl, pH 8.0, and then reduced with 10 mM DTT at 37˚C for 30 min and alkylated with 40 mM iodoacetamide in the dark for 30 min. The resultant proteins were digested with trypsin at a ratio of 1:50 (trypsin/protein w/w) at 37˚C for overnight and then desalted using a SepPak C18 cartridge (Waters Corporation) and dried with a SpeedVac.

Stable isotope dimethyl labeling and strong cation exchange (SCX) fractionation. Desalted peptides were re-suspended in 0.1 M sodium acetate, pH 6.0. Next, 4% formaldehyde (CH_2O, which serves as 'light labeled'), 4% deuterated formaldehyde (CD_2O, which serves as 'Heavy labeled') were added to the peptides extracted from IR rats and sham rats, respectively. After mixing, 0.6 M sodium cyanoborohydride ($NaBH_3CN$) was added and the mixtures were incubated at room temperature (20±2˚C) for 1 h. The samples were then quenched by adding 1% ammonium hydroxide, followed by the addition of 5% formic acid. After labeling, the peptides were mixed at a ratio of 1:1 and desalted prior to separation via SCX chromatography as describe previously (44).

Liquid chromatography-mass spectrometry (LC-MS)/MS and data processing. All ESI-based LC-MS/MS experiments were performed on a TripleTOF 5600+ System coupled with an Ultra 1D Plus nano-liquid chromatography device (SCIEX) as previous reported (45). Dried peptides were dissolved in 0.1% formic acid, 2% acetonitrile and 98% H_2O. Subsequently, samples were loaded onto a C18 trap column (5 μm; 5x0.3 mm; Agilent Technologies, Inc.) at a flow rate of 5 μl/min and eluted from the trap column over the C18 analytic column (75 μm x150 mm; 3 μm particle size, 100 Å pore size; Eksigent Technologies) at a flow rate of 300 nl/min using a 100 min gradient. The mobile phase consisted of two components: Component A comprised 3% DMSO and 97% H_2O with 0.1% formic acid; acomponent B contained 3% DMSO and 97% acetonitrile with 0.1% formic acid. Data was acquired using a

Table I. Primer sequences utilized for reverse transcription-quantitative PCR.

Gene	Forward (5'-3')	Reverse (5'-3')
SOS1	GCTCGCCATTACATCTCCAACCTC	CTTCCTGTGTCAGTGGTGGTGATG
Rptor	TGTCCTGGTCTTCCTGCCTGTG	AGCGTAGTCTCTGAACCTGGTGAG
Washc2c	TGCTGTCTAACACCCAGTTCATT	CGCTCATTGGCATCTTCCTCT
Fry	CCACCCTTCTATCGGTTCACA	GGGCTCGGATCACGTTGCT
Decorin	ACAACCATGAAGGCAACTCTCGTC	GAACACTGCACCACTCGGAGATG
Coro2b	GTGTCTGCTTGCGAGGTCTTCC	GCTCTGTGCCTGGCGTCATG
Gphn	AGTAAAAGATGGCTATGCTGTTCG	CCCGCATCACTTGTCCG
Aspn	AACCAAAGAGCCAGTGAACCC	AAGGTCAACCATTCGAGTATCAA
Lamc1	CTCCATGAAGCAACAGATTACCC	ACTGCCCTCCATACCCCAC

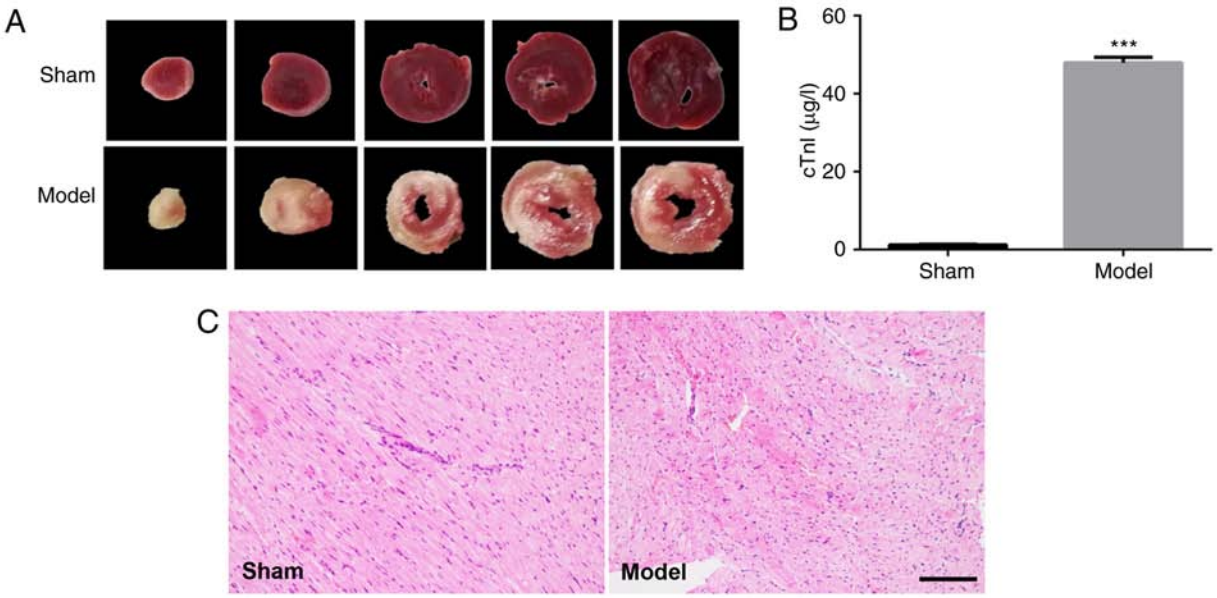

Figure 1. Evaluation of myocardial IR injury. (A) Representative photographs (left panel) in hearts subjected to IR injury. (B) Serum cTnI concentrations in rats with sham or model group. Values are presented as the mean ± standard error of the mean, n=4 rats per group. Mann-Whitney test, ***P<0.0001 vs. the sham group. (C) Representative images of hematoxylin and eosin staining (magnification, x200) from rat left ventricles. IR, ischemia/reperfusion; cTnI, cardiac Troponin I.

spray voltage of 2.3 kV, curtain gas of 20 psi and an interface heater temperature of 150˚C. The information dependent acquisition mode was used to acquire mass spectrometric data. Each scan cycle consisted of one full-scan mass spectrum (with m/z ranging from 350-1,500; ion accumulation time, 250 msec) followed by 40 MS/MS events (m/z ranging from 100-1,500; ion accumulation time, 50 msec). The threshold for MS/MS acquisition activation was set to 120 cps for +2-+5 precursors. Former target ion exclusion was set for 18 sec. The generated raw MS spectra were analyzed with ProteinPilot 4.5 software (SCIEX) using the Paragon algorithm. The uniprot database [*Rattus norvegicus* (Rat), UP000002494] was used. The false discovery rates of the peptide-spectra matches determined by a decoy database search were set to 1.0% for all experimental datasets. Proteins were considered to be successfully identified when at least two correct assigned peptides (95% confidence) were obtained.

Reverse transcription-quantitative PCR. Total RNA from T1-4 segments of the spinal cord tissue was extracted using TRIzol reagent (Invitrogen, Thermo Fisher Scientific, Inc.) according to the manufacturer's protocol. RNA samples were quantified using a spectrophotometer (BioPhotometer; Eppendorf) and then synthesized to cDNA via reverse transcription using the PrimeScript™ RT reagent kit (Takara Bio, Inc.). The temperature protocol of reverse transcription was as follows: 15 min at 37˚C, 5 sec at 85 and 4˚C. cDNA was quantified by quantitative PCR using SYBR-Green Master Mix (Takara Bio, Inc.). The thermocycling conditions for PCR were as follows: 30 sec at 95˚C, followed by 40 cycles of 15 sec at 95˚C, 15 sec at 60˚C and 45 sec at 72˚C. Relative gene expression was determined by normalization to GAPDH using comparative ($2^{-\Delta\Delta Cq}$) method (46). The specific forward and reverse primer sequences (Table I) were designed. The experiments were performed in triplicate. Data are expressed as the mean ± SEM, Mann-Whitney U test compared with the sham group.

Western blotting. Total protein was extracted from T1-4 spinal cord tissues with ice-cold RIPA lysis buffer (Wuhan Boster

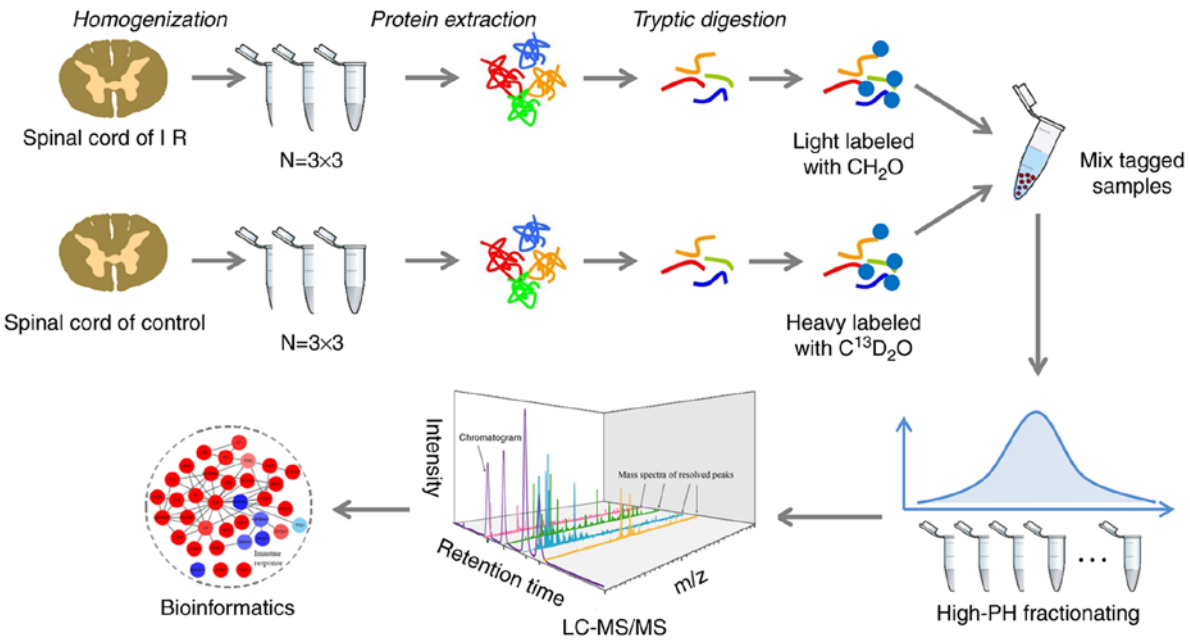

Figure 2. Schematic representation of quantitative proteomics experiment. Proteins were extracted from the spinal cord obtained from 9 rats of I/R and 9 sham rats, respectively. After pooling the protein extracts for every three rats, ischemia/reperfusion and sham samples were reduced, alkylated and tryptic digested, respectively. Then by using stable isotope dimethyl labeling strategy, we performed comparative quantitative proteomics analysis of spinal cord from rats of ischemia/reperfusion (light labeled with CH_2O) and sham rats (heavy labeled with CD_2O). The experiments consist of three biological replicates. LC-MS, liquid chromatography-mass spectrometry. IR, ischemia reperfusion.

Biological Technology, Ltd.). Protein concentrations were determined using the bicinchoninic Protein Assay kit (Wuhan Boster Biological Technology, Ltd.). A total of 30 μg protein samples were separated by SDS-PAGE (5% stacking gel and 10% separating gel) and transferred onto PVDF membranes (EMD Millipore). Then the membrane was blocked in 5% skimmed milk in 0.1% TBST for 1.5 h at room temperature and then incubated overnight at 4˚C with the following primary antibodies: SOS1 (1:500; cat. no. A3272; ABclonal Biotech Co., Ltd.), Coro2b (1:1,000; A16670; ABclonal Biotech Co., Ltd.), Gephyrin (Gphn; 1:500; cat. no. A8572; ABclonal Biotech Co., Ltd.), Rptor (1:200; cat. no. 20984-1-AP; ProteinTech Group, Inc.) and Decorin (1:1,000; cat. no. 14667-1-AP; ProteinTech Group, Inc.). After incubation with horseradish peroxidase-conjugated goat anti-rabbit secondary antibodies (cat. no. A5014; ABclonal Biotech Co., Ltd.) at 1:5,000 concentration for 1.5 h at room temperature. This was followed by protein detection using the ECL Western Blotting Substrate (Thermo Fisher Scientific, Inc.). The mean intensities of selected areas and the areas of these images were calculated using ImageJ software (v.1.8.0_112; National Institutes of Health) and normalized to values of GADPH (1:5,000; ProteinTech). Values were expressed as means ± SEM, Mann-Whitney test compared to the sham group.

Myocardial tissue staining. Each myocardial tissue sample was cut transversely. Hematoxylin and eosin (H&E) staining was used to observe myocardial pathology. After deparaffinization, 4 μm thick sections were immersed in hematoxylin (cat. no. H9627; Sigma-Aldrich; Merck KGaA) for 5-7 min at room temperature, differentiated in 1% acid alcohol for 2-5 sec and stained with 0.5% eosin (cat. no. 71014544; Sinopharm Chemical Reagent Co., Ltd.) for 2 min at room temperature. After rinsing with distilled water for 30 sec, sections were dehydrated with graded alcohol and cleared in xylene. Infarct size was assessed by TTC staining 2 h after reperfusion. After surgery, the hearts were removed and frozen for 20 min at -20˚C, then transversally cut into sections with thickness of ~1 to 2 mm. Tissue sections were incubated in 2% TTC for 10 min in dark conditions at 37˚C and then fixed in 10% formaldehyde overnight at 4˚C. The infarct area was white, while the normal tissues were red.

Bioinformatics. Statistical analysis of the MS results derived from all the experimental groups was performed using Microsoft Office Excel. Pearson correlation analyses was performed to assess the correlation among experimental replicates. Biological Networks Gene Ontology (BiNGO) 3.03 (http://apps.cytoscape.org/apps/bingo) was used to calculate the gene ontology term enrichment of differentia proteins. The analyses were conducted using the default BiNGO *Rattus norvegicus* database. For protein interaction network analysis, the Uniprot functional annotations (http://www.uniprot.org/uniprot) were used to classify the proteins into several clusters. Proteins matched in any cluster of pathways were extracted and submitted to the Search Tool for the Retrieval of Interacting Genes/Proteins (STRING 9.0; https://string-db.org/) to qualify the physical and functional interactions. The proteins and their interactions were then uploaded to Cytoscape (www.cytoscape.org/) for data visualization.

Results

Validation of IR-induced myocardial injury in rats. The histopathological and functional validation analysis was performed to ensure that the IR rats used for the experiments

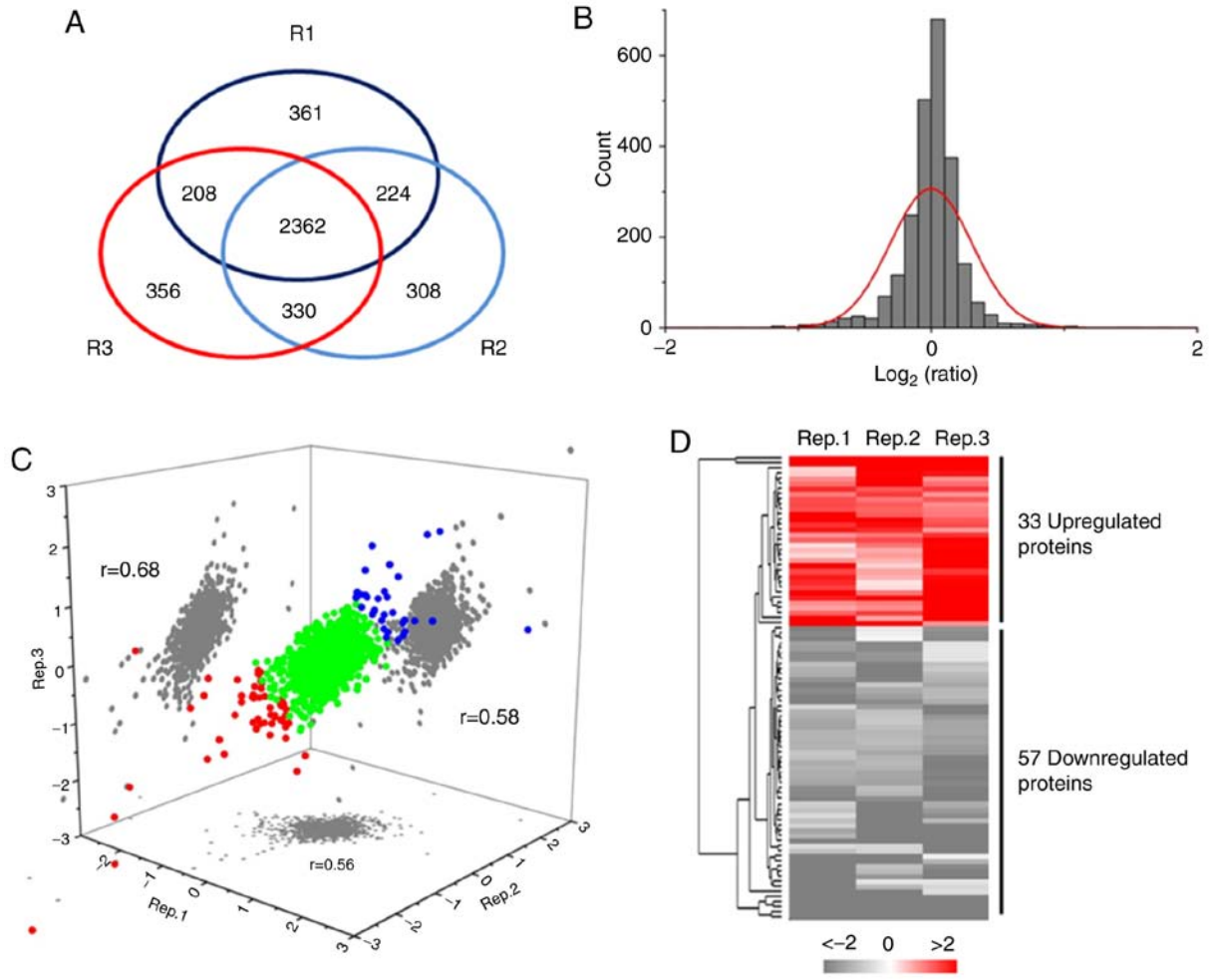

Figure 3. Quantitative proteomics data overview. (A) A total of 4,149 proteins were successfully quantified in the three biological replicates, among which 2,363 proteins were overlapped. (B) Gaussian distribution of the average quantitative data [Log_2 (Ratio)] shared by the three replicates. (C) Pearson correlation analysis of the overlapped proteins shown a good correlation. (D) Heatmap of the 91 differentia proteins (average ratio <0.67 or >1.5-fold).

showed acute myocardial failure. It was observed that 30 min of ischemia resulted in a pale appearance of the ischemia myocardium (Fig. 1A). Serum cardiac troponin cTnI increased significantly (1.211±0.1815 μg/l in sham group, n=4; 47.94±1.368 μg/l, n=4; P<0.001; Fig. 1B). Also, the IR rats showed damaged myocardial cells in the H&E stained heart sections (Fig. 1C). These results verified IR induced myocardial injury in the rats in the study.

Proteomics data overview. To investigate the mechanisms in the spinal cord that respond to myocardial injury, the present study employed a comparative quantitative proteomics approach, based on the stable isotope dimethy labeling strategy, to study the alterations in the spinal cord proteome after acute myocardial IR injury in rats. An experimental flowchart including tissue homogenization, protein extraction, trypsin digestion, chemical labeling and LC-MS/MS processing is shown in Fig. 2. Among the three biological replicates, the present study quantified 4,149 proteins in total, in which 2,362 proteins were shared (Fig. 3A). The gaussian distribution of the shared quantitative data [as log2 (Ratio)] was further analyzed, showing a reasonable ratio distribution (Fig. 3B). The Pearson correlation coefficient analysis showed good repetitiveness among the three biological replicates, as demonstrated by r=0.68, 0.58 and 0.56 (Fig. 3C). All the quantified proteins are summarized in Table SI.

A total of 90 proteins are differentially expressed in the spinal cord after IR injury. To identify the differentially expressed proteins in the spinal cord that are regulated by myocardial injury, a filtering rule was set as previously reported (41,45), to screen those differentially expressed proteins: Proteins with 50% change of ratio in each replicate, or P<0.05 in each replicate and additionally 50% change of average ratio, were considered to be differentially expressed. Among the whole quantitative dataset, 33 spinal cord proteins were found to be upregulated in IR rats, whereas 57 proteins were downregulated (Fig. 3C and D). All the differentially expressed proteins are summarized in Table SII.

To ascertain the functional representation of these differentially expressed proteins, the data were further analyzed based on the gene ontology term enrichment (Fig. S1). The present study found the terms of biological process including axon projection, neurofilaments assembly, microtubule based transport, amino acid metabolism and cell adhesion were enriched among the differentia proteins (Fig. S1A). Molecular function terms including NADPH activity and protein binding and cellular component terms including spiceosomal complex,

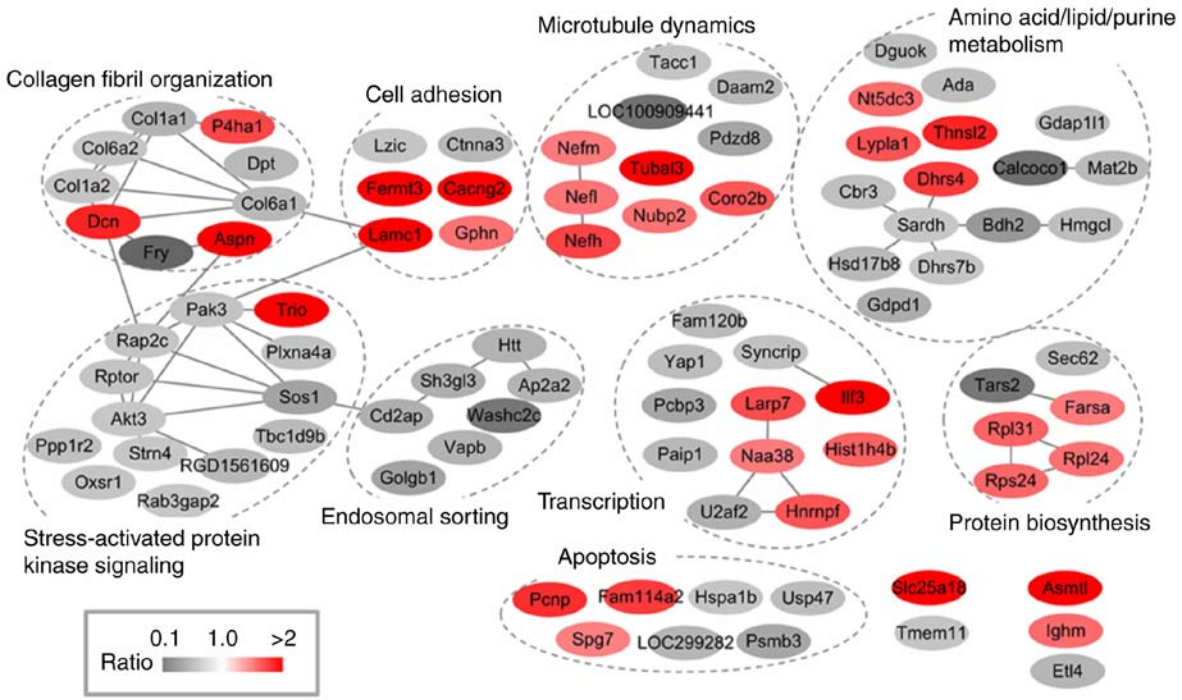

Figure 4. Protein interaction analysis. Interactions among the differentially expressed proteins were obtained by STRING 9.0.

endocytic vesicle and neurofilament were enriched. These results indicate diverse cellular functions were involved in the spinal cord after myocardial injury.

Protein network regulated by IR injury. Considering the possible regulatory network that exists among the differentially expressed proteins, the present study performed protein interaction network based on the STRING database and Uniprot annotations. As shown in Fig. 4, the differentially expressed proteins constitute multiple functional clusters, including collagen fibril organization, cell junction, microtubule dynamics, amino acid/lipid/purine metabolism, stress-activated protein kinase signaling, endosomal sorting, transcription, protein biosynthesis and apoptosis. Several co-regulations possibly exist among these clusters, as the present study found proteins of stress-activated protein kinase signaling and endosomal sorting showed a consistent down-regulatory tendency in IR rats. While upregulatory proteins were mainly found in clusters of cell junction, microtubule dynamics, transcription and protein biosynthesis. These results indicate a complicated response to myocardial injury in the spinal cord.

Alternative evidence supporting the MS findings. To cross-check the reliability of quantitative proteomics, several protein expression levels were further assessed using conventional western blotting and quantitative PCR. A total of five proteins involved in stress-activated protein kinase signaling (Sos1 and Rptor), cell junction (Gphn), collagen fibril organization [Dcn (Decorin)] and microtubule dynamics [Coro2b (Corin2b)], in the regulated protein network, were selected for western blot analysis (Fig. 5). The relative gray value compared with GAPDH of Sos1, Rptor, Gphn, Dcn and Corin2b were 0.6136±0.06747 (n=6), 0.8721±0.1504 (n=4), 1.622±0.2363 (n=5), 1.006±0.1513 (n=5) and 1.245±0.03118 (n=5), respectively. The authors found most of the analyzed proteins were consistent with the MS results except the protein Dcn, which almost did not change in the western blotting results.

Moreover, these five genes and another four genes (Wash2c, Fry, Aspn and Lamc1) were further analyzed by quantitative PCR. As shown in Fig. 6, the results showed that most of the quantitative ratios were consistent with the MS results. These results provide alternative evidences supporting the MS findings.

Discussion

The thoracic spinal cord plays an important role in the regulation of myocardial ischemia-reperfusion injury. By exploring the altered characteristics at three levels (metabolomics, transcriptomics and proteomics) in the thoracic spinal cord under myocardial IR injury, the mechanism of heart-spinal cord neural crosstalk can be further elucidated, which provides a new perspective for clinical intervention alleviating myocardial IR injury by spinal nerve mechanisms in the future.

The present study attempted to systematically profile the proteome-wide alterations of the spinal cord after myocardial IR injury by quantitative proteomics and further analyzed the possible regulatory mechanisms among the various pathways, and protein-interaction networks. The myocardial IR injury rat model first established by cross clamping the LAD for 30-min ischemia and followed by reperfusion for 2 h, as reported previously (47,48), which showed a significant histopathological and functional myocardial injury. Then using the stable isotope dimethyl labeling quantitative proteomics strategy, a total of 2,362 shared proteins with a good distribution and correlation were successfully quantified. Among these proteins, 33 were identified to be upregulated and 57 downregulated proteins in

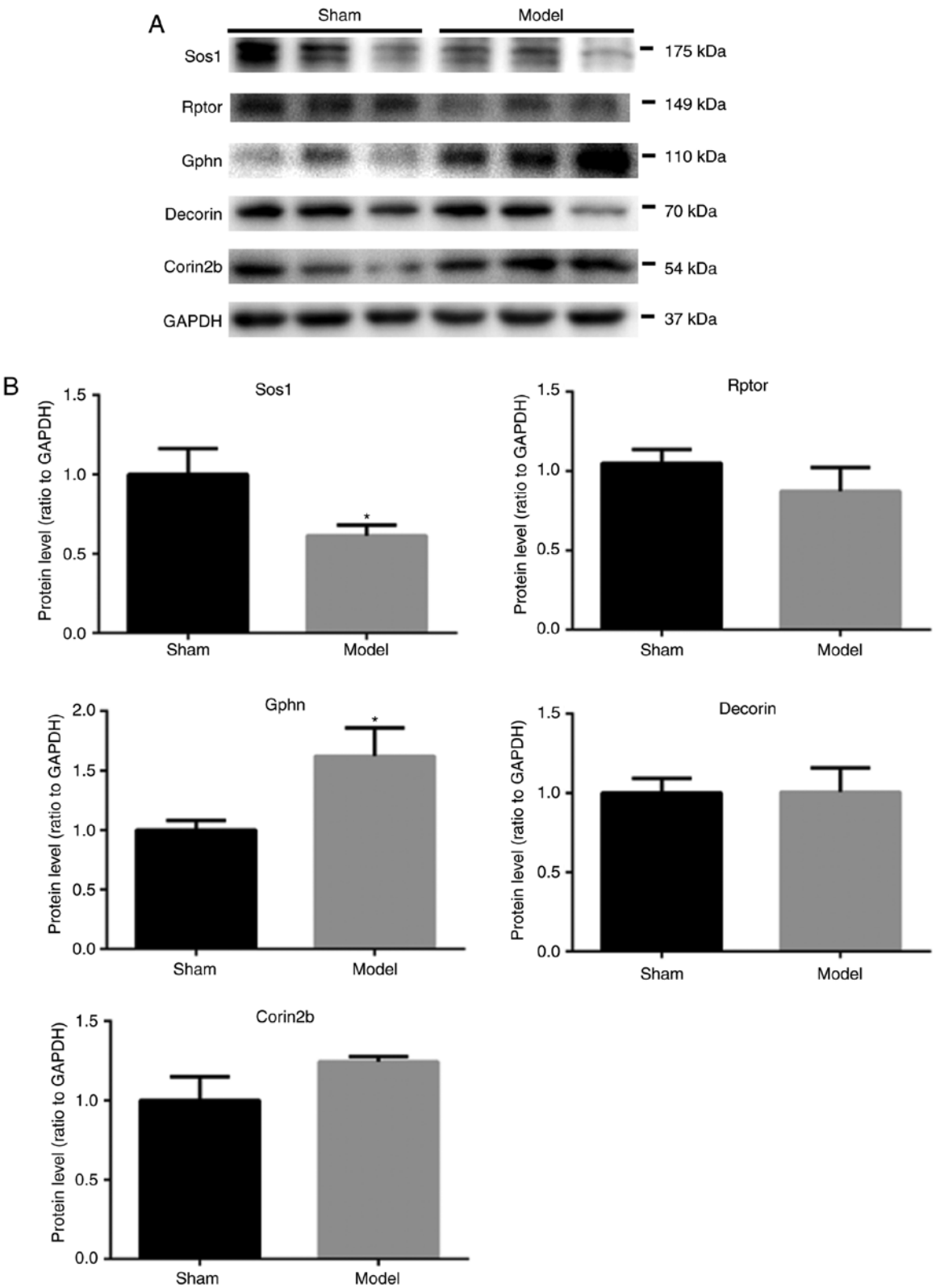

Figure 5. WB analysis of differential proteins. (A) A total of five proteins were selected to be analyzed by WB. (B) Gray value of relative expression levels of Sos1, Rptor, Gphn, Dcn and Corin2b normalized to GAPDH. Most of the analyzed proteins showed a good consistency with the mass spectrometry results except the protein Decorin, which almost not changed in the WB results. Mann-Whitney U test, *P<0.05 was considered statistically significant. WB, western blotting.

the spinal cord after myocardial IR injury, which are involved in various biological processes, molecular function and cellular components. Based on these proteins, the spinal cord protein interaction network regulated by IR injury including apoptosis, microtubule dynamics, stress-activated signaling and cellular metabolism was further established. The cellular protein networks and pathways in spinal cord associated with the myocardial I/R injury are discussed in more detail bellow.

Spinal cord injury especially in the second phase induces cell death, which occurs via apoptosis and autophagy (49,50).

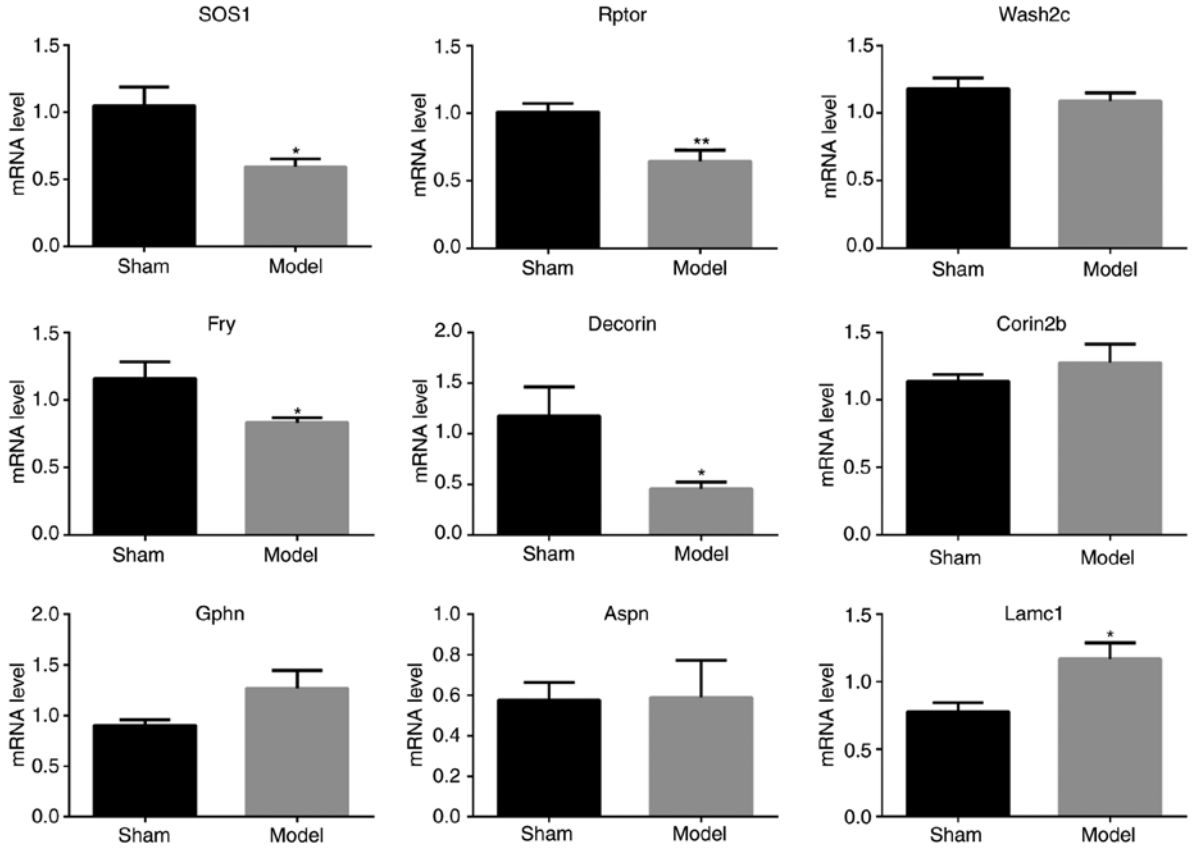

Figure 6. Reverse transcription-quantitative PCR of differential proteins. Values are means ± standard error of the mean (n=6). Mann-Whitney test, *P<0.05 and **P<0.01 vs. the sham group.

As evolutionarily conserved catabolic processes, apoptosis and neuronal autophagy remove those unwanted cytosolic proteins and damaged organelles through the autophagosome/lysosomal pathway (49). The phosphoinositide 3-kinase (PI3K)/protein kinase B (Akt)/mammalian target of rapamycin (mTOR) signaling is reported to play important roles after neuronal injury and can induce apoptosis through the mitochondrial pathway (51,52).

In the present study, proteins of the GTPase that regulates signaling in the spinal cord were identified after myocardial IR injury, including Rap2c, Akt3, Rptor, Sos1 and Pak3 and Strn4, which were all found to be consistently decreased. Previous studies have reported that Rap2c expression was lower in SCII and under hypoxic conditions, and the overexpression of Rap2c could reverse the cell apoptosis induced by hypoxia (53). Akt3 proteins were reported to be degraded as early as 1 h after stroke during brain injury (54). Rptor, as an associated regulatory protein of mTOR complex 1, was found to be decreased in the present study, implying a possible downregulation of mTOR, as suggested by a previous study (55).

Cerebral ischemia induced a cascade of events that may disrupt membrane trafficking pathways including Golgi apparatus-late endosome-lysosome axis, which are important for supplying lysosomal enzymes for cellular apoptosis and autophagy processes (56). Massive buildup of damaged Golgi, transport vesicles and late endosomes takes place over time in neurons destined to die after transient cerebral ischemia or cardiac arrest (57,58).

In the present study, several membrane trafficking related proteins, including Cd2ap, endophilin-A3 (Sh3gl3), huntingtin (Htt), Ap2a3, Wahc2c and Golgb1, were found to all decrease after myocardial IR injury. Cd2ap serves as an adaptor protein and participates in cellular apoptosis via the PI3K/Akt signaling pathway (59). Htt functions as a scaffold for selective macroautophagy (60) and was found to be degraded after ischemic injury, it interacts with Sh3gl3 to function in microtubule-based endocytotic processes (61,62). Additionally, cerebral ischemia was reported to induce mitochondrial membrane permeabilization (56). The present study identified an upregulated protein Spg7, with proteolytic activity involved in the formation and regulation of the mitochondrial permeability transition pore, which was also reported to be regulated during cerebral ischemic injury and treatment (63), and the abnormal expression of which could cause paraplegias (64).

Moreover, microtubule dynamics play important roles in autophagy and apoptotic processes after spinal cord injury, including intracellular trafficking and extracellular matrix remodeling (65,66). The present study found the spinal cord neurofilament proteins Nefl, Nefm, Nefh and protein Tubal3, Nubp2 and Coro2a were upregulated after myocardial IR injury. These results suggested that the microtubule mediated intracellular trafficking in spinal cord were regulated by myocardial IR injury.

After neuron injury, the extracellular matrix (ECM) is degraded and the composition changes, and some molecules become aberrantly expressed or cleaved into bioactive fragments (67). In this study, the collagen type I Col1a1, Col1a2

and collagen type VI Col6a1, Col6a2 were found to be decreased, and the laminin subunit 1 Lamc1 was increased. The prolyl-4-hydroxylase P4ha1, a key cellular oxygen sensor and a regulatory enzyme in the maturation of collagens (68), was found to be increased. Moreover, the collagen binding protein Dcn and Aspn both were increased. Dcn is a proteoglycan constituent of the ECM reported to possess powerful anti-inflammation properties in cardiovascular diseases (69). These results suggested that a possible degradation of the collagen component in ECM of the spinal cord and the collagen metabolism may be involved in the regulation in the spinal cord in response to myocardial IR injury in rats.

Additionally, two neuronal receptor regulatory proteins Cacng2 and Gphn were identified that were both upregulated in the spinal cord of myocardial IR injured rats. Cacng2, also called as stagazin or TRAP-2, is required for inflammation associated AMPA receptor plasticity and involved in nociception within the lamina of the spinal cord (70). Gphn is a scaffold protein responsible for the traffic and synaptic anchoring of $GABA_A$ receptors (71). These results possibly implied special roles for the spinal cord neuronal receptor during myocardial IR injury.

Cellular metabolism including amino acid and lipid metabolism, and protein biosynthesis were also found to be involved in the regulation in the spinal cord after myocardial IR injury. The present study demonstrated that sarcosine dehydrogenase and several of its interacting proteins (Bdh2, Dhrs7b, Hsd17b8 and Cbr3) were downregulated after myocardial IR injury. Moreover, it was also found that some transcription related proteins are regulated in the spinal cord response to myocardial IR injury, including the increased Naa38, larp7 and Hnrnpf. However, the detailed mechanism of these proteins mostly remain rarely investigated.

In conclusion the present study investigated the alterations in the spinal cord that respond to myocardial IR injury in rats using a quantitative proteomics approach. A total of nine differentially expressed spinal cord proteins were identified in the myocardial IR injured rats and the regulated protein networks were further established. The results demonstrated that myocardial IR injury induced regulation of various biological processes in the spinal cord including apoptosis and autophagy, cellular membrane trafficking, extracellular matrix remodeling and some other related biological processes. The present study may provide basis for further detailed clarification of the spinal cord regulatory mechanisms in response to myocardial IR injury.

Acknowledgements

Not applicable.

Funding

This study was supported by grants from the National Natural Science Foundation of P.R. China (grant nos. 81670240 and 81873467 to HX), the National Natural Science Foundation of Hubei Province (grant no. 2016CFB625 to HX), the Medical innovation project in Fujian Province (grant no. 2017-CX-48 to SL) and the Key Research and Development Project of Hainan Province of China (grant no. ZDYF2018115 to DW).

Availability of data and materials

The datasets used and/or analyzed during the current study are available from the corresponding author on reasonable request.

Authors' contributions

HBX and HLZ conceived and designed the study. SYL, QW and ZXL performed the surgical procedures. YJL, QY and ZGH participated in the experimental design. SYL, QY and ZXL performed the experiments. DZW and SYL analyzed the data. HBX and HLZ wrote the manuscript and all authors contributed to the final manuscript. All authors read and approved the final manuscript.

Ethics approval and consent to participate

The present study was approved by the Institutional Ethical Committee of Tongji Hospital, Tongji Medical College, Huazhong University of Science and Technology (grant no. TJ-A20150804).

Patient consent for publication

Not applicable.

Competing interests

The authors declare that they have no competing interests.

References

1. Rahman W, Suzuki R, Webber M, Hunt SP and Dickenson AH: Depletion of endogenous spinal 5-HT attenuates the behavioural hypersensitivity to mechanical and cooling stimuli induced by spinal nerve ligation. Pain 123: 264-274, 2006.
2. Dogrul A, Ossipov MH and Porreca F: Differential mediation of descending pain facilitation and inhibition by spinal 5HT-3 and 5HT-7 receptors. Brain Res 1280: 52-59, 2009.
3. Suzuki R, Rygh LJ and Dickenson AH: Bad news from the brain: Descending 5-HT pathways that control spinal pain processing. Trends Pharmacol Sci 25: 613-617, 2004.
4. Sasaki M, Obata H, Kawahara K, Saito S and Goto F: Peripheral 5-HT2A receptor antagonism attenuates primary thermal hyperalgesia and secondary mechanical allodynia after thermal injury in rats. Pain 122: 130-136, 2006.
5. Kember G, Ardell JL, Shivkumar K and Armour JA: Recurrent myocardial infarction: Mechanisms of free-floating adaptation and autonomic derangement in networked cardiac neural control. PLoS One 12: e0180194, 2017.
6. Kember G, Armour JA and Zamir M: Neural control hierarchy of the heart has not evolved to deal with myocardial ischemia. Physiol Genomics 45: 638-644, 2013.
7. Pan HL, Chen SR, Scicli GM and Carretero OA: Cardiac interstitial bradykinin release during ischemia is enhanced by ischemic preconditioning. Am J Physiol Heart Circ Physiol 279: H116-H121, 2000.
8. Pan HL, Longhurst JC, Eisenach JC and Chen SR: Role of protons in activation of cardiac sympathetic C-fibre afferents during ischemia in cats. J Physiol 518: 857-866, 1999.
9. Wolfrum S, Nienstedt J, Heidbreder M, Schneider K, Dominiak P and Dendorfer A: Calcitonin gene related peptide mediates cardioprotection by remote preconditioning. Regul Pept 127: 217-224, 2005.
10. Szallasi A and Blumberg PM: Vanilloid (Capsaicin) receptors and mechanisms. Pharmacol Rev 51: 159-212, 1999.
11. Blair RW, Weber RN and Foreman RD: Responses of thoracic spinothalamic neurons to intracardiac injection of bradykinin in the monkey. Circ Res 51: 83-94, 1982.

12. Kuo DC, Oravitz JJ and Degroat WC: Tracing of afferent and efferent pathways in the left inferior cardiac nerve of the cat using retrograde and transganglionic transport of horseradish peroxidase. Brain Res 321: 111-118, 1984.
13. White JC: Cardiac pain: Anatomic pathways and physiologic mechanisms. Circulation 16: 644-655, 1957.
14. Pan HL and Chen SR: Myocardial ischemia recruits mechanically insensitive cardiac sympathetic afferents in cats. J Neurophysiol 87: 660-668, 2002.
15. Ding X, Ardell JL, Hua F, McAuley RJ, Sutherly K, Daniel JJ and Williams CA: Modulation of cardiac ischemia-sensitive afferent neuron signaling by preemptive C2 spinal cord stimulation: Effect on substance P release from rat spinal cord. Am J Physiol Regul Integr Comp Physiol 294: R93-R101, 2008.
16. Foreman RD: Mechanisms of cardiac pain. Annu Rev Physiol 61: 143-167, 1999.
17. Hua F, Ardell JL and Williams CA: Left vagal stimulation induces dynorphin release and suppresses substance P release from the rat thoracic spinal cord during cardiac ischemia. Am J Physiol Regul Integr Comp Physiol 287: R1468-R1477, 2004.
18. Steagall RJ, Sipe AL, Williams CA, Joyner WL and Singh K: Substance P release in response to cardiac ischemia from rat thoracic spinal dorsal horn is mediated by TRPV1. Neuroscience 214: 106-119, 2012.
19. Kang YM, Yang ZM, Ma Y, Lei JH, Yan N, Su YK and Francis J: TNF-alpha contributes to cardiac nociception in myocardial infarction. Circulation (81st Annual Scientific Session of the American-Heart-Association) 118: S296-S296, 2008.
20. Ding X, Mountain DJ, Subramanian V, Singh K and Williams CA: The effect of high cervical spinal cord stimulation on the expression of SP, NK-1 and TRPV1 mRNAs during cardiac ischemia in rat. Neurosci Lett 424: 139-144, 2007.
21. Gourine A and Gourine AV: Neural mechanisms of cardioprotection. Physiology (Bethesda) 29: 133-140, 2014.
22. Evonuk KS, Prabhu SD, Young ME and DeSilva TM: Myocardial ischemia/reperfusion impairs neurogenesis and hippocampal-dependent learning and memory. Brain Behav Immun 61: 266-273, 2017.
23. Dou M, Ma Z, Cheng X, Zou G, Xu Y, Huang C, Xiong W, He S and Zhang Y: Intrathecal lentivirus-mediated RNA interference targeting nerve growth factor attenuates myocardial ischaemia-reperfusion injury in rat. Br J Anaesth: Aug 2, 2019 (Epub ahead of print).
24. Pan XC, Li ZX, Wu DZ, Li SY, Xiang HB and Song YT: Mapping changes of whole brain blood flow in rats with myocardial ischemia/reperfusion injury assessed by positron emission tomography. Curr Med Sci 39: 653-657, 2019.
25. Singh H, Merry AF, Ruygrok P and Ruttley A: Treatment of recurrent chest pain in a heart transplant recipient using spinal cord stimulation. Anaesth Intensive Care 36: 242-244, 2008.
26. Southerland EM, Milhorn DM, Foreman RD, Linderoth B, DeJongste MJ, Armour JA, Subramanian V, Singh M, Singh K and Ardell JL: Preemptive, but not reactive, spinal cord stimulation mitigates transient ischemia-induced myocardial infarction via cardiac adrenergic neurons. Am J Physiol Heart Circ Physiol 292: H311-H317, 2007.
27. Jiang L, Hu J, He S, Zhang L and Zhang Y: Spinal neuronal NOS signaling contributes to morphine cardioprotection in ischemia reperfusion injury in rats. J Pharmacol Exp Ther 358: 450-456, 2016.
28. Lu Y, Hu J, Zhang Y and Dong C: Spinal neuronal NOS activation mediates intrathecal fentanyl preconditioning induced remote cardioprotection in rats. Int Immunopharmacol 19: 127-131, 2014.
29. Lu Y, Hu J, Zhang Y, Dong CS and Wong GT: Remote intrathecal morphine preconditioning confers cardioprotection via spinal cord nitric oxide/cyclic guanosine monophosphate/protein kinase G pathway. J Surg Res 193: 43-51, 2015.
30. Iwamoto T, Bai XJ and Downey HF: Preconditioning with supply-demand imbalance limits infarct size in dog heart. Cardiovasc Res 27: 2071-2076, 1993.
31. Huang C, Wang J, Wang N, Du F, Xiong W, Qian J, Zhong K, Cai A, Xu S, Huang J, *et al*: Effect of myocardial ischemic preconditioning on ischemia-reperfusion stimulation-induced activation in rat thoracic spinal cord with functional MRI. Int J Cardiol 285: 59-64, 2019.
32. Liu BW, Li ZX, He ZG, Liu C, Xiong J and Xiang HB: Altered expression of target genes of spinal cord in different itch models compared with capsaicin assessed by RT-qPCR validation. Oncotarget 8: 74423-74433, 2017.
33. Chen M, Li ZX, Wang Q and Xiang HB: Altered expression of differential genes in thoracic spinal cord involved in experimental cholestatic itch mouse model. Curr Med Sci 38: 679-683, 2018.
34. Wang Q, Li ZX, Liu BW, He ZG, Liu C, Chen M, Liu SG, Wu WZ and Xiang HB: Altered expression of differential gene and lncRNA in the lower thoracic spinal cord on different time courses of experimental obstructive jaundice model accompanied with altered peripheral nociception in rats. Oncotarget 8: 106098-106112, 2017.
35. Liu T, He Z, Tian X, Kamal GM, Li Z, Liu Z, Liu H, Xu F, Wang J and Xiang H: Specific patterns of spinal metabolites underlying alpha-Me-5-HT-evoked pruritus compared with histamine and capsaicin assessed by proton nuclear magnetic resonance spectroscopy. Biochim Biophys Acta Mol Basis Dis 1863: 1222-1230, 2017.
36. He ZG, Liu BW, Li ZX, Liu C and Xiang HB: Altered expression profiling of spinal genes modulated by compound 48/80 in a mouse itch model. J Anesth Perioper Med 4: 220-224, 2017.
37. Wang Q, He ZG, Li ZX, Li SY, Chen YL, Feng MH, Hong QX and Xiang HB: Bioinformatics analysis of gene expression profile data to screen key genes involved in cardiac ischemia-reperfusion injury. Int J Clin Exp Med 11: 4955-4966, 2018.
38. Wang Q, Li ZX, Li YJ, He ZG, Chen YL, Feng MH, Li SY, Wu DZ and Xiang HB: Identification of lncRNA and mRNA expression profiles in rat spinal cords at various time-points following cardiac ischemia/reperfusion. Int J Mol Med 43: 2361-2375, 2019.
39. Wang Q, Li ZX, Li YJ, Manyande A, Li SY, Feng MH, Wu DZ and Xiang HB: Alterations in amino acid levels and metabolite ratio of spinal cord in rat with myocardial ischemia-reperfusion injury by proton magnetic resonance spectroscopy. Am J Transl Res 11: 3101-3108, 2019.
40. Zeng HL, Yu FL, Zhang Z, Yang Q, Jin S, He X, Chen X, Shen Y, Cheng L, Guo L and Xu F: Quantitative proteomics study of host response to virulent and attenuated pseudorabies virus infection in mouse brain. Biochim Biophys Acta Proteins Proteom 1866: 307-315, 2018.
41. Zeng HL, Yang Q, Du H, Li H, Shen Y, Liu T, Chen X, Kamal GM, Guan Q, Cheng L, *et al*: Proteomics and metabolomics analysis of hepatic mitochondrial metabolism in alcohol-preferring and non-preferring rats. Oncotarget 8: 102020-102032, 2017.
42. Murry CE, Jennings RB and Reimer KA: Preconditioning with ischemia: A delay of lethal cell injury in ischemic myocardium. Circulation 74: 1124-1136, 1986.
43. Hickman DL and Johnson SW: Evaluation of the aesthetics of physical methods of euthanasia of anesthetized rats. J Am Assoc Lab Anim Sci 50: 695-701, 2011.
44. Zeng HL, Rao X, Zhang LK, Zhao X, Zhang WP, Wang J, Xu F and Guo L: Quantitative proteomics reveals olfactory input-dependent alterations in the mouse olfactory bulb proteome. J Proteomics 109: 125-142, 2014.
45. Jiang DS, Zeng HL, Li R, Huo B, Su YS, Fang J, Yang Q, Liu LG, Hu M, Cheng C, *et al*: Aberrant epicardial adipose tissue extracellular matrix remodeling in patients with severe ischemic cardiomyopathy: Insight from comparative quantitative proteomics. Sci Rep 7: 43787, 2017.
46. Livak KJ and Schmittgen TD: Analysis of relative gene expression data using real-time quantitative PCR and the 2(-Delta Delta C(T)) method. Methods 25: 402-408, 2001.
47. Foley LS, Fullerton DA, Bennett DT, Freeman KA, Mares J, Bell MT, Cleveland JC Jr, Weyant MJ, Meng X, Puskas F and Reece TB: Spinal cord ischemia-reperfusion injury induces erythropoietin receptor expression. Ann Thorac Surg 100: 41-46, 2015.
48. Wang Y, Pang QJ, Liu JT, Wu HH and Tao DY: Down-regulated miR-448 relieves spinal cord ischemia/reperfusion injury by up-regulating SIRT1. Braz J Med Biol Res 51: e7319, 2018.
49. Balsam LB: Spinal cord ischemia-reperfusion injury: MicroRNAs and mitophagy at a crossroads. J Thorac Cardiovasc Surg 154: 1509-1510, 2017.
50. Beattie MS, Farooqui AA and Bresnahan JC: Review of current evidence for apoptosis after spinal cord injury. J Neurotrauma 17: 915-925, 2000.
51. Wang Z, Zhou L, Zheng X, Chen G, Pan R, Li J and Liu W: Autophagy protects against PI3K/Akt/mTOR-mediated apoptosis of spinal cord neurons after mechanical injury. Neurosci Lett 656: 158-164, 2017.
52. Jung SY, Kim DY, Yune TY, Shin DH, Baek SB and Kim CJ: Treadmill exercise reduces spinal cord injury-induced apoptosis by activating the PI3K/Akt pathway in rats. Exp Ther Med 7: 587-593, 2014.

53. Qiao Y, Peng C, Li J, Wu D and Wang X: Spinal cord ischemia-reperfusion causes damage of neurocyte by inhibiting RAP2C. Neurol Res 39: 877-884, 2017.
54. Xie R, Cheng M, Li M, Xiong X, Daadi M, Sapolsky RM and Zhao H: Akt isoforms differentially protect against stroke-induced neuronal injury by regulating mTOR activities. J Cereb Blood Flow Metab 33: 1875-1885, 2013.
55. Hwang JY, Gertner M, Pontarelli F, Court-Vazquez B, Bennett MV, Ofengeim D and Zukin RS: Global ischemia induces lysosomal-mediated degradation of mTOR and activation of autophagy in hippocampal neurons destined to die. Cell Death Differ 24: 317-329, 2017.
56. Yuan D, Liu C and Hu B: Dysfunction of membrane trafficking leads to ischemia-reperfusion injury after transient cerebral ischemia. Transl Stroke Res 9: 215-222, 2018.
57. Liu CL, Ge P, Zhang F and Hu BR: Co-translational protein aggregation after transient cerebral ischemia. Neuroscience 134: 1273-1284, 2005.
58. Zhang F, Liu CL and Hu BR: Irreversible aggregation of protein synthesis machinery after focal brain ischemia. J Neurochem 98: 102-112, 2006.
59. Ren Q and You Yu S: CD2-associated protein participates in podocyte apoptosis via PI3K/Akt signaling pathway. J Recept Signal Transduct Res 36: 288-291, 2016.
60. Rui YN, Xu Z, Patel B, Chen Z, Chen D, Tito A, David G, Sun Y, Stimming EF, Bellen HJ, *et al*: Huntingtin functions as a scaffold for selective macroautophagy. Nat Cell Biol 17: 262-275, 2015.
61. Ralser M, Nonhoff U, Albrecht M, Lengauer T, Wanker EE, Lehrach H and Krobitsch S: Ataxin-2 and huntingtin interact with endophilin-A complexes to function in plastin-associated pathways. Hum Mol Genet 14: 2893-2909, 2005.
62. Hughes AC, Errington R, Fricker-Gates R and Jones L: Endophilin A3 forms filamentous structures that colocalise with microtubules but not with actin filaments. Brain Res Mol Brain Res 128: 182-192, 2004.
63. Choi TM, Yun M, Lee JK, Park JT, Park MS and Kim HS: Proteomic analysis of a rat cerebral ischemic injury model after human cerebral endothelial cell transplantation. J Korean Neurosurg Soc 59: 544-550, 2016.
64. Thal DR, Züchner S, Gierer S, Schulte C, Schöls L, Schüle R and Synofzik M: Abnormal paraplegin expression in swollen neurites, τ- and α-synuclein pathology in a case of hereditary spastic paraplegia SPG7 with an Ala510Val mutation. Int J Mol Sci 16: 25050-25066, 2015.
65. He M, Ding Y, Chu C, Tang J, Xiao Q and Luo ZG: Autophagy induction stabilizes microtubules and promotes axon regeneration after spinal cord injury. Proc Natl Acad Sci USA 113: 11324-11329, 2016.
66. Hellal F, Hurtado A, Ruschel J, Flynn KC, Laskowski CJ, Umlauf M, Kapitein LC, Strikis D, Lemmon V, Bixby J, *et al*: Microtubule stabilization reduces scarring and causes axon regeneration after spinal cord injury. Science 331: 928-931, 2011.
67. Gaudet AD and Popovich PG: Extracellular matrix regulation of inflammation in the healthy and injured spinal cord. Exp Neurol 258: 24-34, 2014.
68. Myllyharju J: Prolyl 4-hydroxylases, master regulators of the hypoxia response. Acta Physiol (Oxf) 208: 148-165, 2013.
69. Vu TT, Marquez J, Le LT, Nguyen ATT, Kim HK and Han J: The role of decorin in cardiovascular diseases: More than just a decoration. Free Radic Res 52: 1210-1219, 2018.
70. Sullivan SJ, Farrant M and Cull-Candy SG: TARP γ-2 Is required for inflammation-associated AMPA receptor plasticity within Lamina II of the spinal cord dorsal horn. J Neurosci 37: 6007-6020, 2017.
71. Costa JT, Mele M, Baptista MS, Gomes JR, Ruscher K, Nobre RJ, de Almeida LP, Wieloch T and Duarte CB: Gephyrin cleavage in in vitro brain ischemia decreases GABAA receptor clustering and contributes to neuronal death. Mol Neurobiol 53: 3513-3527, 2016.